

***In situ* electrical characterization of phase transformations in Si during indentation**

J. E. Bradby and J. S. Williams

Department of Electronic Materials Engineering, Research School of Physical Sciences and Engineering, The Australian National University, Canberra, ACT 0200, Australia

M. V. Swain

Biomaterials Science Research Unit, Department of Mechanical and Mechatronic Engineering and Faculty of Dentistry, The University of Sydney, Eveleigh, NSW 1430, Australia

(Received 13 August 2002; published 28 February 2003)

An *in situ* electrical characterization technique is used to study details of the deformation behavior of crystalline silicon during nanoindentation. The experimental arrangement involves the measurement of current flow through a reverse-biased Schottky diode and exploits a sharp transition from a Schottky to an Ohmic contact that accompanies the formation of a metallic Si-II phase directly under the indenter. This electrical technique is particularly sensitive to the nature and extent of the local Si-I to Si-II phase transformation and allows such changes to be directly correlated with features in nanoindentation load-unload curves, using both spherical and Berkovich indenters. Interestingly, for spherical indentation, the onset of a transformation to a metallic Si-II phase is observed before the so-called “pop-in” event occurs during loading. Furthermore, after the “pop-in” event, fine structure in the electrical behavior suggests that extrusion of the ductile metallic Si-II phase from under the indenter may occur when the transformed area exceeds that of the indenter contact. Indeed, the *in situ* electrical measurements have provided considerable insight into the evolution of deformation processes during indentation loading and unloading of Si. During unloading, metallic Si-II transforms to less electrically conducting phases of Si. We suggest that, although Si-III and Si-XII are the preferred low pressure phases during pressure release, as diamond anvil studies show, *a*-Si is often obtained during fast unloading rates as a result of a high kinetic barrier to nucleation of the crystalline phases. Furthermore, we suggest that the pop-out occurs for slow unloading rates as a result of spontaneous nucleation and growth of the crystalline phases at a critical pressure.

DOI: 10.1103/PhysRevB.67.085205

PACS number(s): 62.20.-x, 72.80.Cw, 61.72.-y, 62.20.Fe

I. INTRODUCTION

The complex mechanisms of mechanical deformation in crystalline silicon have been a topic of extensive research over the past decade.^{1–15} High pressure diamond-anvil studies have shown that Si undergoes a series of phase transformations under isostatic loading.^{1,2} At a pressure of 11.3–12.5 GPa, diamond-cubic Si-I undergoes a 22% increase in density to form a β -Sn phase, Si-II.¹ Si-II is a metallic phase of Si and hence has the electronic and mechanical properties of a metal and not a semiconductor. This phase is not stable at ambient pressure and, hence, will transform to another form of Si on pressure release.² Diamond-anvil studies have reported the formation a rhombohedral (r8) Si-XII phase and a body-centered-cubic (bc8) Si-III structure after quenching from Si-II. The final structure of the remnant phase has been found to depend on the rate of pressure release.^{1,2}

Nanoindentation can induce pressures of the magnitude needed to cause phase transformations in Si.^{3–7} However, in contrast to diamond-anvil cell measurements, indentation loading also induces high shear stress which has been reported to lower the threshold for the onset of a phase transformation.¹⁶ Furthermore, nanoindentation load-unload data of crystalline Si has been reported to show discontinuities in both the loading and unloading sections of the curve.^{5–11} A discontinuity on loading (a “pop-in” event) has only been conclusively observed for indents made with spherical indenters.^{6–9} In contrast, a discontinuity on unloading (a “pop-out” event) has been reported for both spherical

and pointed indenters.^{5–11} Although nanoindentation data contains much information regarding the physical deformation mechanisms occurring during loading and unloading, the interpretation of this data is not straightforward. Indeed, the physical cause of the pop-in and pop-out events has not been unambiguously resolved.^{5–11} Therefore, in order to more fully understand the deformation processes, additional characterization techniques, that probe the structure and phase of the deformed material, have been used.

After indentation, the surface of residual indent impressions in crystalline Si has been extensively imaged using optical microscopy, atomic force microscopy (AFM), and scanning electron microscopy (SEM).^{3–7} These measurements have reported the observation of extruded material around the indent suggestive of the fact that a ductile Si-II phase may flow under load. Moreover, the microstructure beneath the surface has been examined using transmission electron microscopy (TEM), and phase transformed regions have been observed directly under the surface of the indent.^{3,8–10,14,15} Furthermore, Raman microspectroscopy has been used to analyze the residual indent impressions and has identified a number of high pressure phases after indentation.^{9,11–13} We have previously correlated both cross-sectional transmission electron microscopy (XTEM) and Raman microspectroscopy observations with nanoindentation data in order to improve the understanding of both the evolution of and mechanisms involved in the deformation of Si.^{8,9} Using XTEM we observed small regions of phase transformed material in indents made at loads below the

pop-in threshold.⁹ Similar experiments using both Raman microspectroscopy and XTEM have shown a correlation between the unloading rate and the structure of the remnant phase. Si-III and Si-XII were identified on slow rates of unloading and an amorphous-Si (*a*-Si) phase under rapid unloading conditions.^{8,11–13} Although the correlation of nanoindentation with AFM, SEM, XTEM, and Raman microspectroscopy has provided further insights into the deformation of Si, these techniques are all *ex situ* and hence characterize only the final structure after deformation is complete.

In situ electrical measurements were first performed by Gridneva *et al.*¹⁷ In these experiments, the resistance between metal contacts evaporated onto the surface of crystalline Si was measured during indentation. The resistance was found to decrease during loading and recover to its initial value on unloading. It was proposed that the decrease in the resistance during loading was due to the formation of the metallic Si-II phase which electrically connected the two metallic contacts allowing increased current flow. Similar experiments by Clarke *et al.*³ showed that it was not necessary to make bridging indents between the contacts in order to achieve a drop in the resistance. Simply indenting on one contact would also cause a drop in resistance. It was proposed that the formation of metallic Si during loading facilitated the conversion of the contact from Schottky (rectifying) to Ohmic.³ Further work by Pharr *et al.*⁵ showed that the change in the resistance of Si during indentation could be dominated by changes in contact resistance rather than phase transformation to a metallic Si phase. Simulations of nanoindentation loading in crystalline Si were recently performed by Smith *et al.*¹⁸ In these simulations, phase transformations and changes in the electrical resistance during loading were shown to agree well with the experimental results of Pharr *et al.*⁵ In addition, further *in situ* electrical measurements were recently reported by Mann *et al.* using a conductive indenter tip.¹⁰ This work showed that the transformation from a Schottky to an Ohmic contact during loading was consistent with the formation of the metallic Si phase from the nanoindentation data. The assertion was also made that the reverse transformation from the metallic Si-II phase was not instantaneous but, rather, was quite sluggish.

Despite the above *in situ* measurements, to date it has not been possible to correlate the detailed features of the nanoindentation load-unload data with changes in electrical properties during indentation. In this paper we employ an *in situ* electrical characterization technique that is particularly sensitive to the nature and extent of phase transformations occurring in crystalline Si under the indenter. Our technique specifically relies on the conversion of an Al-Si contact during indentation from Schottky to Ohmic due to such transformations. The Si structure used consists of a high resistivity epitaxial layer on a substrate with a low resistivity and a large area Al-Si Schottky contact fabricated on the epitaxial layer. This structure provides particular sensitivity to the onset of a phase transformation directly under the indenter. Our detailed electrical measurements during indentation are correlated with nanoindentation data and previously reported Raman and XTEM measurements in order to more fully un-

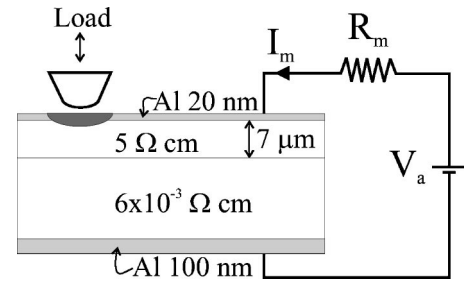


FIG. 1. Schematic of experimental setup. The Si structure consists of a $\sim 7 \mu\text{m}$ epilayer of high resistance Si ($5 \Omega \text{ cm}$) grown on bulk Si with a very low resistance ($6 \times 10^{-3} \Omega \text{ cm}$). Al was evaporated onto both sides and a circuit was connected across the sample.

derstand the deformation processes that occur during the nanoindentation of Si.

II. EXPERIMENTAL

The (100) Si samples used in this study were *p*-type boron doped. The structure of the samples consisted of a $\sim 7 \mu\text{m}$ epilayer of high resistivity ($5 \Omega \text{ cm}$) Si on a substrate with a low resistivity ($6 \times 10^{-3} \Omega \text{ cm}$). Aluminum layers were evaporated onto both the front and back surfaces of the sample. During Al evaporation, the edges of the Si were covered using a mask to avoid conduction around the sides of the sample. The thickness of the Al layers were typically in the range of ~ 20 and ~ 100 nm for the front (epilayer) and back (substrate) side of the sample, respectively. Subsequent electrical characterization confirmed that a Schottky (rectifying) contact was formed at the Al-to-epilayer interface. Schottky contacts form as a result of the lightly doped epilayer that produces a significant depletion layer thickness under the contact and hence acts as a barrier to current flow (in reverse bias). In contrast to the Al-to-epilayer interface, the Al-to-substrate interface formed an Ohmic contact because of the much higher carrier concentration in the substrate compared to that of the epilayer.

The Si structure was placed in series with a $1 \text{ k}\Omega$ resistor (R_m) as shown in Fig. 1. A dc voltage V_a (typically set to 1 V) was applied across the circuit so that the Schottky contact (on the epilayer) was placed under reverse bias. Prior to indentation loading, the effective resistance across the sample (under reverse bias of 1 V) was $\sim 75 \text{ k}\Omega$ and the voltage across R_m (V_m) had a value of $\sim 0.01 \text{ V}$. The magnitude of V_m increases as the sample resistance decreases, with a corresponding increase in the current flow across the sample. Hence, V_m is effectively a measure of the total circuit current I_m . During indentation this value was monitored as a function of time.

The area of the Schottky contact (front side) was $\sim 0.75 \text{ cm}^2$. During indentation loading at a typical load of 100 mN , the area of contact between the spherical indenter we used and the sample was in the order of $\sim 4 \mu\text{m}^2$. Therefore, due to the large ratio between the area of the Schottky contact and the indenter contact area, our measurement was sensitive only to dramatic changes in the electronic (contact) properties of the small region of material under the indenter.

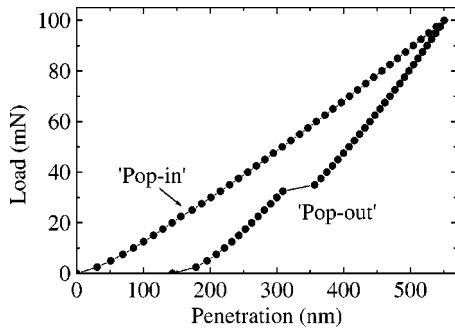


FIG. 2. Load-unload curve of ~ 20 nm of Al on crystalline Si showing “pop-in” and “pop-out” events. Loading conditions: Maximum load 100 mN, 40 steps, spherical indenter of ~ 4.2 μm radius.

The transformation of a small region of the Schottky contact to an Ohmic contact would provide such a dramatic effect. Following a phase transformation of the semiconducting Si-I to the metallic Si-II phase under the indenter, if the contact region was converted to an Ohmic contact, the current density in this region would be expected to increase by orders of magnitude (as we show later). Hence, the total current I_m would increase significantly.

Indentations were made with an Ultra-Micro Indentation System-2000 (UMIS) on the Schottky contact as shown in Fig. 1 at ambient pressure and room temperature. An SEM was used to characterize both a spherical (radius ~ 4.2 μm) and a pointed (Berkovich) indenter. The UMIS was calibrated using fused silica of known material properties. A series of indentations was made on the silicon sample with both spherical and Berkovich indenters at loads of up to 100 mN. Two loading routines were used: a continuous load-unload cycle, and the load partial-unload method developed by Field and Swain.¹⁹ During indentation, the load applied by the UMIS was measured together with the current I_m as a function of time. This allowed the electrical characteristics and nanoindentation measurements to be accurately correlated. Subsequent SEM examination of the residual indent impressions showed no evidence of delamination, cracking or rupture of the thin Al layer after indentation.

III. RESULTS

The mechanical response of the Al/Si structure to nanoindentation loading is shown in Fig. 2. This plot shows the load versus penetration depth for an indent made with a spherical indenter of ~ 4.2 μm radius loaded to 100 mN. There is essentially no difference between the loading behavior shown in this figure and that made on bare Si except for a slight increase in the maximum depth of penetration for the Al/Si system (< 20 nm) as a result of deformation of the extremely soft but thin Al layer. Discontinuities can be seen in both the loading and unloading sections of this plot. The pop-in event on the loading section of the curve occurs ~ 25 mN (Ref. 20) and the pop-out event on unloading at ~ 35 mN.

The increase in the current through the Al/Si structure during indentation loading is shown in Fig. 3. This figure shows

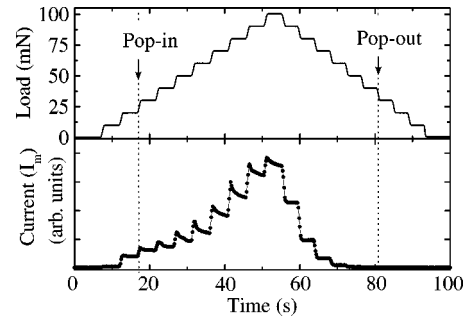


FIG. 3. Applied load and current as a function of time during indentation loading in crystalline Si. Loading conditions: Continuous load-unload cycle, maximum load 100 mN, 10 steps, spherical indenter of ~ 4.2 μm radius. The load at which the pop-in and pop-out events occur is indicated. The current is shown on a linear scale with arbitrary units.

both the applied indentation load and current (I_m) as a function of time for a continuous load-unload cycle with a spherical indenter loaded to 100 mN. The load versus time plot (top curve) shows the details of the continuous loading cycle. At each step in the cycle the load is first sharply increased (or decreased) and then held at a constant magnitude for ~ 2 s until the next increment. Despite the fact that this is actually a somewhat discontinuous loading process we will refer to it as the continuous load cycle. This Fig. 3 shows the load increasing to a maximum of 100 mN in 10 steps (loading), and then decreasing to zero applied load in a further 10 steps (unloading). Corresponding to these loading increments, the magnitude of the current can be seen to increase with the applied load in clearly definable steps. This observed increase in current is quite significant when the small area of the indentation is considered. From absolute current measurements, the current density is $\sim 2 \times 10^{-2}$ mA/cm² through the large area Schottky contact and $\sim 2 \times 10^6$ mA/cm² through the small area of the indent after transformation.

Figure 3 also shows that, for most loading increments, the current through the sample exhibits an initial sharp increase (spike), during the loading portion of the load step, and then a slight decrease during the constant load part of each loading increment. This behavior was observed to occur for each loading increment with the possible exception of the initial step. Creep (i.e., an increase in depth with constant load) measurements showed that holding the maximum load (100 mN) for 20 sec resulted in $< 0.5\%$ decrease in the mean contact pressure. Therefore, creep is not the reason for the decrease in the current following the initial spike as the load is held constant. Alternative explanations for this effect will be discussed later in the paper. In addition, Fig. 3 shows that the onset of additional current through the sample occurs at a load of ~ 15 mN, i.e., before the pop-in event has occurred. In contrast to the loading part of the cycle, on unloading, the magnitude of the current falls dramatically with decreasing load. At a load of ~ 50 mN (well before the pop-out event has occurred) the current returns to a value close to that before loading. It is interesting to note that, during unloading, the magnitude of the current is relatively constant be-

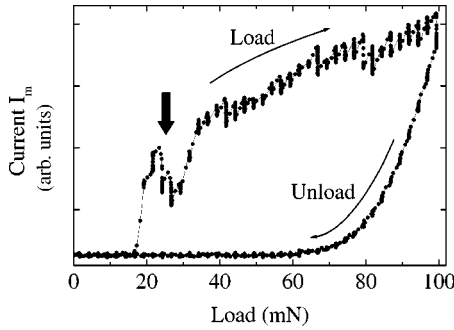


FIG. 4. Current versus applied load during indentation of Si. Loading conditions: Continuous load-unload cycle, maximum load 100 mN, 40 steps, spherical indenter of $\sim 4.2 \mu\text{m}$ radius. The arrow indicated the load at which the pop-in event was observed to occur. The current is shown on a linear scale with arbitrary units.

tween unloading steps. This is in contrast to the behavior observed on loading, where a noticeable spike in the magnitude of the current occurs at each step.

The current through the sample (I_m in Fig. 1) versus applied load during indentation is shown in more detail in Fig. 4. In this plot the maximum load of 100 mN is applied in 40 increments in order to highlight the comparison of electrical characteristics with load. Note that this is the same loading condition used for the load-unload curve shown in Fig. 2. As the load is increased, the current only increases significantly above a threshold load of ~ 17 mN. Note a subsequent drop in the magnitude of the current at ~ 24 mN (indicated in this figure by an arrow). This is very close to the load at which the pop-in event has been observed to occur (see Fig. 2), the significance of which is discussed later in the paper. As loading continues, the current can be seen to increase with each loading step noting the “spike” at the onset of each loading increment. On unloading, the current can be observed to fall consistently as the indenter is withdrawn, reaching its pre-load value at ~ 60 mN.

In Fig. 5 we examine the effect of the indenter geometry on the electrical properties of indented Si. Figures 5(a) and 5(b) show the current and load as a function of time for a spherical and Berkovich indenter, respectively. Both indents were made using a continuous load-unload cycle, with 20 steps to a maximum load of 100 mN. Spherical indentation exhibits an initial increase in current at a load of ~ 22 mN while, in the case of the Berkovich indenter, the change occurs almost immediately after loading (< 5 mN). On unloading, the current decreases to the preindentation level at similar loads (~ 65 mN).

Figure 6 shows the applied load and resulting changes in current for a load partial-unload indentation cycle loaded to a maximum of 100 mN. Figure 6(a) treats an indent made with unloading to 50% of the load at each step and Fig. 6(b) the case of unloads to 80%. On each partial unloading step, the current can be seen to fall rapidly as the load is decreased. When the unloading fraction is set to 50% [Fig. 6(a)], the current returns to the preindentation level at each unloading step. In contrast, this is not observed when the unload fraction is set to 80% [Fig. 6(b)], with the current remaining above preloading levels during each unloading step. As this

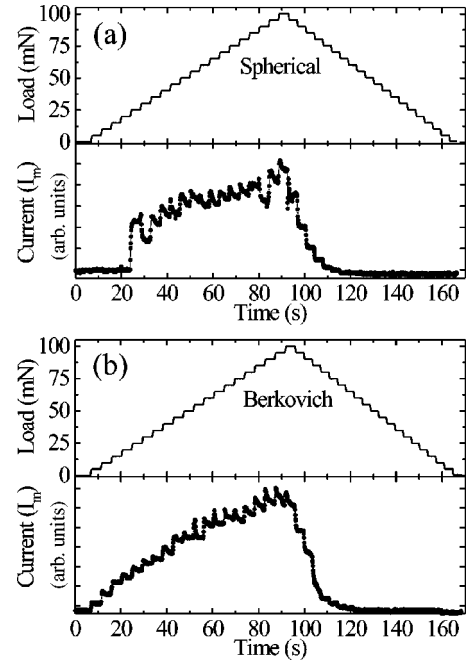


FIG. 5. Applied load and current as a function of time during nanoindentation of a single indentation. Loading conditions: Continuous load-unload cycle, maximum load of 100 mN, 20 steps. (a) Spherical indenter of $\sim 4.2 \mu\text{m}$ radius. (b) Berkovich indenter. The current is shown on a linear scale with arbitrary units.

type of loading cycle is a form of cyclic loading, these results highlight the reversibility of the phase transformation (as we discuss later). In addition, it is interesting to note that there is no observed spike in the magnitude of the current during the first step in the current in both plots (denoted by arrows), in contrast to the subsequent loading increments, a feature we will also discuss later in the paper. Indeed, in a separate measurement we observed that reindentation on previously indented spots showed that the current always increases again on loading (although the initial increase is at a higher load for subsequent indents) and decreases to background levels on unloading even after repeated indentation at the same position on the sample.

IV. DISCUSSION

A. Electrical behavior

Before discussing the details of the indentation-induced deformation of Si, we will first attempt to interpret the electrical behavior. Prior to indentation, a Schottky contact was formed at the Al-to-epilayer interface, preventing significant current flow through the circuit under reverse bias conditions. An equivalent circuit representing this configuration is shown in Fig. 7 where the right branch across the sample indicates the reverse bias situation in which the reverse current is limited by a large effective resistance R_{rev} defined by Eq. (1)

$$R_{\text{rev}} = R_{\text{Sc}} + \left(\frac{\rho_e t_e}{A_{\text{rev}}} \right) + \left(\frac{\rho_s t_s}{A_{\text{rev}}} \right). \quad (1)$$

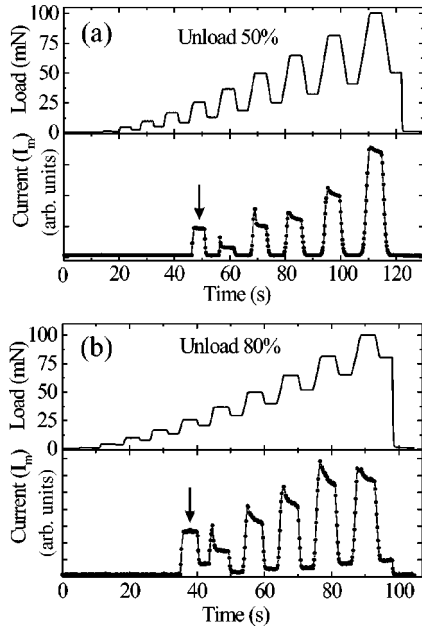


FIG. 6. Applied load and current as a function of time during indentation loading in crystalline Si. Loading conditions: Partial load-unload cycle, maximum load 100 mN, 10 steps, spherical indenter of $\sim 4.2 \mu\text{m}$ radius. (a) Partial unload to 50% of each loading step showing resistivity increases to background levels on unloading. (b) Partial unload to 80% of each loading step showing resistivity remains below background levels on unloading after ~ 40 mN. The arrows indicate the first step at which the current can be observed to increase. The current is shown on a linear scale with arbitrary units.

Here, R_{Sc} is the effective Schottky resistance under reverse bias and the following terms are the series resistance of the epilayer and the underlying substrate, respectively. In this equation, ρ is the resistivity, t is the thickness of the layer, A

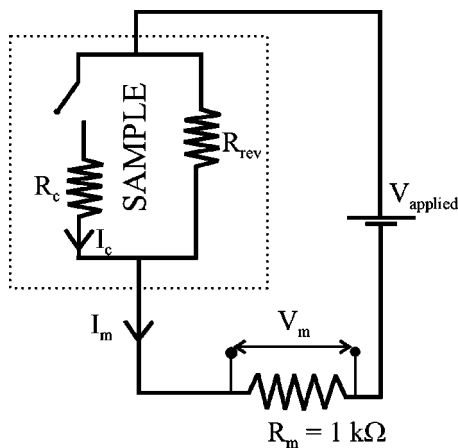


FIG. 7. Circuit simulating the behavior of the Si structure before indentation (as shown with switch open) and during indentation (switch closed). R_{rev} is the resistance of the sample in reverse bias, R_c is the resistance of the contact during indentation, and the voltage V_m was measured across the resistor R_m . I_m is the current flowing through R_m and hence is the total current in the circuit and I_c is the current flowing through R_c as indicated.

is the contact area under reverse bias, and the subscripts “e” and “s” refer to the epilayer and substrate properties, respectively. Note that the effective resistance of the backside, large-area Ohmic contact is considered to be negligible. Equation (1) assumes that the contact area (0.75 cm^2) is large compared with the sample thickness (0.07 cm) and hence any spreading (resistance) terms relating to the epilayer and the substrate can be neglected. Under reverse bias conditions, according to Eq. (1), the resistance R_{rev} is dominated by R_{Sc} , since both $(\rho_e t_e / A_{\text{rev}})$ and $(\rho_s t_s / A_{\text{rev}})$ have small values of $\sim 5 \times 10^{-3} \Omega$ and $\sim 6 \times 10^{-4} \Omega$, respectively, whereas R_{Sc} has a value of the order of 75 k Ω . Hence, the measured value of $R_{\text{rev}} \approx R_{Sc}$ in this case.

As stated earlier, the significant increase in the current on loading must indicate that the Schottky contact is transformed to an Ohmic contact in the small region under the indenter. We assume that this behavior is caused by a pressure-induced transformation to the metallic Si-II phase immediately under the Al layer. In this case, the barrier height between the Al and the underlying metallic Si-II material is now negligible and the Schottky contact is effectively converted to an Ohmic contact under the indenter. If we assume that there is no effective Schottky barrier between different crystalline phases of Si (Si-II and Si-I), significantly increased current will now flow under reverse bias if the resistivity of the Si across the sample is sufficiently low. Thus, before loading the reverse current is restricted by the high effective resistance (R_{Sc}) of the large ($\sim 0.75 \text{ cm}^2$) Schottky contact whereas, after phase transformation during loading, a large increase in current is obtained through the small area under the indenter. As previously stated, the current density through the region under the indenter is orders of magnitude greater than the surrounding nontransformed regions (from $\sim 2 \times 10^{-2} \text{ mA/cm}^2$ to $\sim 2 \times 10^6 \text{ mA/cm}^2$). Hence, Eq. (1) no longer defines the resistance that controls the current flow I_m in the circuit of Fig. 7.

When an Ohmic contact is formed under the indenter, we can envisage the switch in the left sample branch in Fig. 7, being closed and an additional current to flow, in parallel with the reverse-bias current through the large area Schottky contact. We can define an additional resistance, R_c for this Ohmic branch as given by Eq. (2):

$$R_c = R_{\text{Ohm}} + \left(\frac{\rho_e}{2\pi r} \tan^{-1} \frac{2t_e}{r} \right) + \left(\frac{\rho_s}{2\pi r} \tan^{-1} \frac{2t_s}{r} \right). \quad (2)$$

Here R_{Ohm} is the specific contact resistance of the Ohmic contact and the second and third terms are the spreading resistance²¹ for the epilayer and the substrate, respectively, with ρ_e , ρ_s , t_e , t_s having the same values as in Eq. (1), and r is the radius of the Ohmic contact (i.e., the transformed region under the indenter). If we assume that the current through the reverse-biased Schottky contact (the right sample branch in Fig. 7) is unchanged by the formation of a very small Ohmic contact under the indenter, then the additional current on loading flows only through the Ohmic contact and hence is controlled by the sample resistance R_c as indicated in Fig. 7. Now, according to Eq. (2) for a situation where r

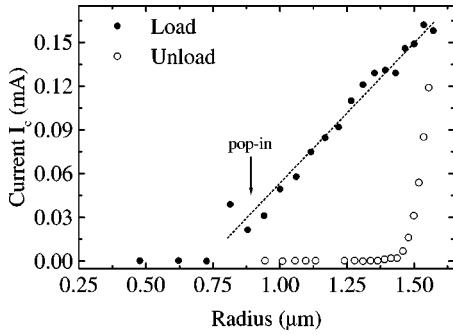


FIG. 8. Additional current during indentation versus the contact radius of the indenter with the sample. The contact radius between the indenter and the sample was calculated using the radius of the indenter ($\sim 4.2 \mu\text{m}$) and the depth of penetration. The arrow indicates the load at which the pop-in event has been observed to occur. Loading conditions: Continuous load-unload cycle, maximum load of 100 mN, 20 steps.

($< 2 \mu\text{m}$) is smaller than the layer thickness ($t_e \approx 7 \mu\text{m}$) the (spreading) resistance terms are both roughly inversely proportional to the radius of the Ohmic contact. We note that these latter two terms in Eq. (2) (under our experimental conditions) will sum to the order of several $\text{k}\Omega$'s (at a maximum load of 100 mN). Estimation of the magnitude of R_{Ohm} is more difficult and may not be negligible with respect to the spreading terms: we note that the value of R_{Ohm} will be inversely proportional to the contact area (i.e., $\propto 1/r^2$).

In Fig. 8 we plot the additional current through R_c (i.e., I_c) as a function of the indenter contact radius for both the loading and unloading cycle up to a maximum load of 100 mN. The linear relationship on loading, noting that the dotted line in Fig. 8 is a least-square fit excluding the points prior to transformation, may suggest that the current through the Ohmic contact is controlled by the spreading terms in Eq. (2) (i.e., R_{Ohm} is negligible in comparison). However, over the limited contact range of this experiment, I_c is also found to exhibit a reasonably linear relationship with contact area (i.e., $\propto 1/r^2$). Hence, it is unclear at this stage which of the terms in Eq. (2) controls the additional current following phase transformation. Finally, we observe, as before, that the reduction in current flow on unloading is extremely abrupt. This result suggests that the current is turned off rapidly and is not sensitive to the sequence of phase changes that presumably occur during unloading. Both the loading and unloading behavior are now discussed in terms of other (*ex situ*) structural observations below.

B. Loading

On indentation loading, the isostatic pressure induced by a spherical indenter is at a maximum directly under the indenter.²² Once this pressure increases past $\sim 11 \text{ GPa}$ the phase transformation to the metallic Si-II phase is initiated. In our case for an indenter of radius $\sim 4.2 \mu\text{m}$ analytical simulations²³ indicate that the maximum isostatic compressive stress will exceed 11 GPa when the load reaches $\sim 15.5 \text{ mN}$. This is in good agreement with the electrical

measurements (see Fig. 4) that indicate that the onset of a phase transformation is around 17 mN. We note that the maximum in the isostatic pressure occurs under the indenter at the center of the contact area and decreases radially outward. Modeling indicates that the area under the indenter that exceeds the critical isostatic pressure (i.e., transformed area) scales with the contact area.^{6,22} This in turn would imply that the indenter contact area should correspond to the area of the Ohmic contact, which is basically the assumption made in the previous subsection.

In the Al/Si structure used in our configuration, the transformation will occur in the epilayer just beneath the Al layer. Previous *ex situ* XTEM and Raman microspectroscopy observations of indents made under comparable loading and unloading conditions to those presented here, showed the presence of phase transformed material after indentation.⁸⁻¹⁵ Previous *ex situ* TEM (Refs. 3,10,14,15) and Raman microspectroscopy¹¹⁻¹³ observations of indents, showed the presence of phase transformed material after indentation. Under comparable indenter geometry and loading conditions to those presented in this current study, our previous work has shown that the maximum depth of the transformed region is 600 nm (at a load of 80 mN with a spherical indenter of $\sim 4.2 \mu\text{m}$).⁸ In addition to the transformed material directly under the indenter, there are slip bands, attributable to shear, that propagate $< 2 \mu\text{m}$ below the surface. Thus, all the deformation induced by the indentation loading can reasonably be expected to remain confined to the $7 \mu\text{m}$ epilayer of the Si structure.

Focusing now on details of the electrical behavior, we observe in Figs. 3 and 4 that the onset of increased current and hence the phase transformation is initiated before the pop-in event is observed. This directly supports previous XTEM studies that showed small regions of phase-transformed material in residual indent impressions loaded below the pop-in threshold.⁹ Based on this result we previously suggested that the pop-in event occurs when the transformed material flows out from under the indenter. This would occur when the lateral extent of the transformed region exceeds the diameter of contact between the indenter and the sample. Furthermore AFM and SEM observations of indent impressions in crystalline Si show extruded material at the edge of the residual indent impression (after the pop-in event).⁹ This behavior is further evidence for the proposal that this Si-II transformed material is squeezed out during loading. We now examine in more detail the loading sequence and use the details of the *in situ* electrical data to support our model.

A schematic of the sequence of events induced under the indenter is illustrated in Fig. 9. Figure 9(a) shows the early stages of loading before the pop-in event but after the initiation of the transformation to Si-II in a region under the indenter that is totally constrained within the contact diameter. With further loading, the diameter of the transformed region (Si-II) increases until it exceeds the indenter contact diameter. Once this occurs the ductile Si-II can then flow out from under the indenter as illustrated in Fig. 9(b). In the extruded region, the isostatic pressure will immediately decrease and the Si-II in this region may then be transformed

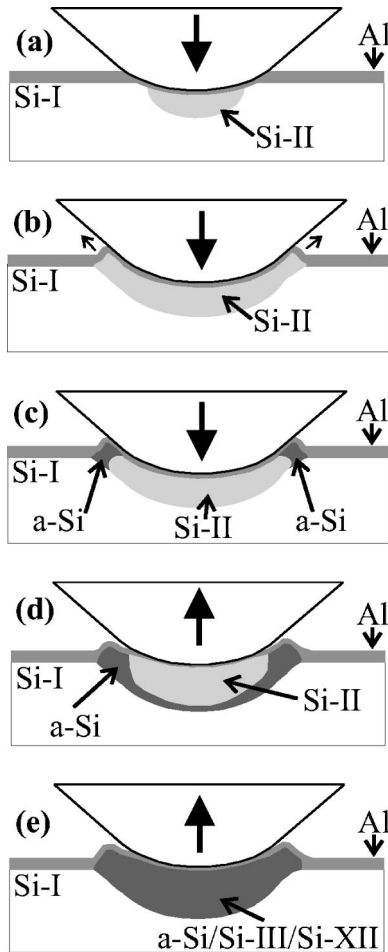


FIG. 9. Schematic of the deformation sequence occurring during indentation. (a) On loading, initiation of the transformation of semi-conducting Si-I to the metallic Si-II phase. (b) With further loading the transformed region expands outside the diameter of constraint of the indenter resulting in the extrusion of material from under the indenter (pop-in). (c) After extrusion the material in this region transforms to an amorphous phase. (d) As unloading commences, the metallic Si-II phase begins to transform to a -Si. (e) As unloading continues the mean contact pressure beneath the indenter decreases to a level at which the bulk of Si-II is no longer stable. The bulk of Si-II then transforms to either a -Si, Si-III, or Si-XII depending on the rate of pressure release.

into another low pressure phase since Si-II is not stable at pressures significantly below the threshold for the initial transformation.^{1,10} This behavior may provide one explanation for the “spike” in the measured current that is observed immediately following each loading step after the pop-in event. The spike could correspond to the increased area of the transformed material that is extruded from under the indenter. However, the current will immediately drop during the constant load part of each loading step (see Figs. 3, 5, and 6) when some of the newly transformed (Si-II) in the extruded region transforms to a low pressure phase (say to a -Si) as illustrated in Fig. 9(c). However, a transient capacitance effect which could contribute to the current decay across a capacitor formed by the Al- a -Si contact might also lead to a current spike. We will return to this issue below. If

material extrusion is the explanation for the spike, this illustrates the sensitivity, of the electrical measurements to time-dependent changes in the surface area of the metallic Si-II phase during each loading step.

In discussing the nature of the subsequent phase that the extruded Si-II transforms to, we note that previous observations of indents made with rapid unloading rates have revealed the formation of an amorphous Si phase.^{8,13} Hence, since the extrusion process involves rapid pressure release, the resultant phase of this extruded material is likely to be amorphous. In this regard, it is interesting to note that XTEM studies of indentation-induced transformations in Si do show that the edges of the transformed zone are indeed a -Si, even when the main volume of the transformed zone (after unloading) consists of other phases such as Si-III and Si-XII.⁸ Hence, we propose that the extrusion process during loading will effectively limit the area of metallic Si-II material to a zone under the indenter, except for a short time immediately after loading (the current spike). Thus, the extrusion process after pop-in will cause the Ohmic contact area to closely correspond to the indenter contact area, further validating the starting assumption made earlier in the previous section, namely, that the Ohmic contact area scales with the indenter radius.

Another significant observation from the electrical data that warrants further comment is the fact that the loading step at which the measured current is first observed to increase is not characterized by a spike in the magnitude of the current. This can be most clearly seen in the load partial-unload data shown in Fig. 6 (see arrow in both plots). Here, the current over the entire duration of the first loading step after the onset of transformation remains constant. This is most consistent with the expected behavior prior to the pop-in event, where no transformed material is extruded and the metallic Si-II area under the indenter should remain constant with time [see Fig. 9(a)]. Furthermore, it suggests that a transient capacitance effect which should be observed at all steps which show a current increase, is not the explanation for the current spike. In addition, this behavior prior to the pop-in event is not observable for indents made with a Berkovich indenter, since the small diameter of the indenter tip and the rapidly changing radial isostatic pressure will effectively negate any significant constraint to extrusion of the transformed volume from under the indenter. Therefore, all of the fine details in the electrical measurements during loading are entirely consistent with the transformation/extrusion and re-transformation model that we propose above.

C. Unloading

On unloading, the current is observed to fall dramatically in clearly defined steps as the indenter is withdrawn (see Figs. 3–6). Indeed, as can be seen in Fig. 3, the current drops back to the preindentation levels well before the pop-out event occurs. The pop-out event (for Si) is widely interpreted to be as a result of the large change in volume that occurs with the transformation from the metallic Si-II phase to less dense phases. For example, a -Si is approximately 24% less

dense (than Si-II) and Si-III is 14% less dense compared with Si-II. This transformation from Si-II to a less dense phase will be favored when the mean contact pressure under the indenter drops to a level at which Si-II is no longer stable.^{6-8,10} It is clear therefore that our electrical measurements are not sensitive to the large volume changes that appear to characterize the phase transformation on unloading. Nevertheless, the transformations to lower density phases on unloading might be expected to begin in regions in which the isostatic pressure first drops below the critical level for stability of metallic Si-II. The interface between the metallic Si-II and the underlying Si-I epilayer is where this may first occur during the initial stages of unloading. This is illustrated schematically in Fig. 9(d), which shows a thin continuous layer of a low pressure phase, most likely *a*-Si as we discuss below, that disconnects underlying Si-I from metallic Si-II. When such a continuous layer (of a higher resistivity phase) reaches a critical thickness, the contact may no longer exhibit Ohmic behavior and the magnitude of the current across the sample will revert to its value before loading commenced. Hence, only a small fraction of the volume of the Si-II need transform to a continuous, nonmetallic phase before the current reverts to its preloading levels.

Further evidence that the subsequent transformation process (i.e., resultant structure after the transformation from metallic Si-II to lower pressure phases) severely impedes the current flow was obtained from sequential indentations made on the same position on the sample. It was noted that the onset of current increase observed during subsequent loading cycles occurred only when a higher load was reached. This suggests that the majority of the retransformed material from the previous loading cycle needed to be transformed back to metallic Si-II before our electrical measurements were sensitive to the presence of any metallic Si-II phase. Hence, whereas our experimental setup is extremely sensitive to details of phase transformations during loading of Si-I, it is not particularly sensitive to behavior on unloading. We need now to explore how the transformation to the lower pressure phases subsequently evolves [Fig. 9(e)].

From load-unload and electrical data, Mann *et al.*¹⁰ concluded that the transformation from the metallic Si-II phase on pressure release is slow compared with the unloading rate. Others have noted that both the observation of the pop-out event and the nature of the end phases depend on the unloading rate.^{8,11,13} For example, the Raman study of Domnich *et al.*¹¹ found that no pop-out event was observed when the remnant microstructure of the indents was amorphous. Based partly on these earlier observations and partly on our present data, we propose the following. As soon as unloading begins, the Si-II material starts to transform to a less dense phase that is initially *a*-Si. If the unloading rate is fast, the Si-II can transform entirely to amorphous Si in a relatively continuous manner (albeit more slowly than the unloading rate). Under such a situation, the unloading section of the load-penetration curve will not exhibit a pop-out event. However, if the unloading rate is slow enough, the Si-II may transform at a particular (critical) pressure to the thermodynamically preferred Si-III and Si-XII phases, which may spontaneously nucleate within Si-II. We propose that there is a kinetic bar-

rier to nucleation of such phases. A manifestation of such a nucleation-limited behavior may be that, if the pressure release is too fast, the random low-pressure phase, *a*-Si, will result instead. The implication here is that there may not be a nucleation barrier for *a*-Si within Si-II. However, if Si-III and Si-XII phases do nucleate, their growth will be rapid at lower pressures where Si-II is unstable, thus giving rise to the observed pop-out event on unloading. This proposed behavior may also explain the absence of *a*-Si in diamond anvil experiments, where the much slower pressure release rate per unit volume of Si-II may readily allow nucleation of the preferred (lower free-energy) crystalline Si-III and Si-XII phases.

V. CONCLUSIONS

The Si epilayer structure used in this study has enabled a detailed *in situ* examination of the indentation-induced deformation of crystalline Si. The sensitivity of our experimental configuration to changes in the electrical properties of the sample during loading was exploited to explore fine detail in the nanoindentation data. On loading, the onset of the transformation to the metallic Si-II phase was consistently detected prior to the observation of the pop-in event. This suggested that the pop-in event may be caused by the sudden extrusion of the ductile metallic Si-II phase once this transformed region extends beyond the constraint of the indenter. Consistent with this transformation and extrusion model, fine details in the electrical data such as the spike in the current observed at each loading increment after pop-in, were correlated with transformations between Si-I, Si-II, and high resistivity phases. The load-partial-unload measurements clearly show that the indentation-induced changes in the electrical properties are reversible during further loading cycles. In addition, the extrusion process was found to effectively limit (after the pop-in event) the region of transformed metallic Si-II to the indenter contact area. As the indenter was withdrawn, a sharp decrease in the current flow was observed, as a thin layer of Si-II transformed to a high-resistivity, low-pressure, phase such as *a*-Si. Finally, we suggest that the pop-out event on unloading occurs when crystalline Si-III and Si-XII phases spontaneously nucleate and rapidly grow on unloading. We propose that the formation of these phases is nucleation limited. Hence, the pop-out event can be suppressed if the unloading rate is fast resulting in the formation of only the random *a*-Si phase.

ACKNOWLEDGMENTS

The authors would like to thank and acknowledge Professor C. Jagadish of the Department of Electronic Materials Engineering at The Australian National University for his helpful discussions of these results and Martin Conway for his assistance with the electronic and computer equipment used in this experiment.

- ¹J. Z. Hu, L. D. Merkle, C. S. Menoni, and I. L. Spain, *Phys. Rev. B* **34**, 4679 (1986).
- ²R. O. Piltz *et al.*, *Phys. Rev. B* **52**, 4072 (1995).
- ³D. R. Clarke, M. C. Kroll, P. D. Kirchner, R. F. Cook, and B. J. Hockey, *Phys. Rev. Lett.* **60**, 2156 (1988).
- ⁴G. M. Pharr, W. C. Oliver, and D. S. Harding, *J. Mater. Res.* **6**, 1129 (1991).
- ⁵G. M. Pharr, W. C. Oliver, R. F. Cook, P. D. Kirchner, M. C. Kroll, T. R. Dinger, and D. R. Clarke, *J. Mater. Res.* **7**, 961 (1992).
- ⁶E. R. Weppelmann, J. S. Field, and M. V. Swain, *J. Mater. Res.* **8**, 830 (1993).
- ⁷J. S. Williams, Y. Chen, J. Wong-Leung, A. Kerr, and M. V. Swain, *J. Mater. Res.* **14**, 2338 (1999).
- ⁸J. E. Bradby, J. S. Williams, J. Wong-Leung, M. V. Swain, and P. Munroe, *J. Mater. Res.* **16**, 1500 (2001).
- ⁹J. E. Bradby, J. S. Williams, J. Wong-Leung, M. V. Swain, and P. Munroe, *Appl. Phys. Lett.* **77**, 3749 (2000).
- ¹⁰A. B. Mann, H. Van, D. J. B. Pethica, and T. Weihs, *J. Mater. Res.* **15**, 1754 (2000).
- ¹¹V. Domnich, Y. Gogotsi, and S. Dub, *Appl. Phys. Lett.* **76**, 2214 (2000).
- ¹²A. Kailer, Y. G. Gogotsi, and K. G. Nickel, *J. Appl. Phys.* **81**, 3057 (1997).
- ¹³Y. G. Gogotsi, V. Domnich, S. N. Dub, A. Kailer, and K. G. Nickel, *J. Mater. Res.* **15**, 871 (2000).
- ¹⁴I. Zarudi and L. C. Zhang, *Tribol. Int.* **32**, 701 (1999).
- ¹⁵H. Saka and S. Abe, *J. Electron Microsc.* **46**, 45 (1997).
- ¹⁶J. J. Gilman, *Philos. Mag. B* **67**, 207 (1993).
- ¹⁷I. V. Gridneva, Y. V. Milman, and V. I. Trefilov, *Phys. Status Solidi A* **14**, 117 (1972).
- ¹⁸G. S. Smith, E. B. Tadmor, and E. Kaxiras, *Phys. Rev. Lett.* **84**, 1260 (2000).
- ¹⁹J. S. Field and M. V. Swain, *J. Mater. Res.* **8**, 297 (1993).
- ²⁰The position of the “pop-in” event can be clearly seen by taking the derivative of the load-unload curve. It can also be observed directly from the load-unload curve by looking along the line of the data.
- ²¹E. H. Rhoderick and R. H. Williams, *Metal-Semiconductor Contacts* (Oxford University Press, Oxford, 1988).
- ²²D. Tabor, *The Hardness of Metals* (Oxford University Press, Oxford, 1951).
- ²³T. Chudoba and N. Schwarzer, SCISOFT ELASTICA Version 1.01, TU Chemnitz, 1999.